Nano World Journal

https://doi.org/10.17756/nwj.2023-s1-054

Research Article

Open Access

Experimental Analysis on the Implementation of the Thermoacoustic Refrigeration System Using Working Medium as Air

Sajid Siddiqui* and Akash Langde

Department of Mechanical Engineering, Anjuman College of Engineering and Technology, Nagpur, Maharastra, India

***Correspondence to:**
Sajid Siddiqui
Department of Mechanical Engineering, Anjuman College of Engineering and Technology, Nagpur, Maharastra, India.
E-mail: sajids@anjumanengg.edu.in

Received: November 24, 2022
Accepted: April 16, 2023
Published: April 18, 2023

Citation: Siddiqui S, Langde A. 2023. Experimental Analysis on the Implementation of the Thermoacoustic Refrigeration System Using Working Medium as Air. *NanoWorld J* 9(S1): S277 -S281.

Published by United Scientific Group

Abstract

Thermoacoustic refrigeration is a relatively recent technology that has gained notoriety in the scientific community in the past few years. It involves producing low temperatures with the aid of acoustic sound waves. A thermoacoustic refrigeration system is an appliance that transfers heat via a solid medium characterized as a stack in a resonator tube employing acoustic sound energy as an input. Temperature disparity established across the stack is what determines how well a thermoacoustic refrigerator works. The stack is the thermoacoustic system's most crucial component. The stack, which is composed of Mylar and shaped like a honeycomb, is utilized in the present experimental investigation. Using a mix of set independent and set dependent variables, the experimental data and system analysis were conducted. Air was employed as the system's working medium, and varied pressures and resonant frequencies were applied in order to determine the performance parameters that would yield the best results for the design. The findings are shown, and they support the idea that the stack and its associated parameters play a crucial role in the thermoacoustic refrigeration system's ability to work at its best. The analysis provided offers suggestions for improving thermoacoustic refrigerators' effectiveness, which is still lacking because of their comparatively modest accomplishment. The performance coefficient of the system can also be improved by adjusting other factors like the resonant frequency and the medium of the resonator tube.

Keywords

Thermoacoustic refrigeration, Stack, Resonating medium, Coefficient of performance

Introduction

Thermoacoustic refrigeration describes procedures where sound acoustic energy is converted into heat energy, resulting in the temperature differential needed for refrigeration. The scientific world has recently focused a lot of emphasis on this capability of turning sound energy into a temperature differential [1, 2]. Thermoacoustic refrigeration systems use sound to reduce the temperature of a low-temperature area and increase the temperature of a high-temperature area. In addition to their ability to be environmentally benign, thermoacoustic systems are also becoming more popular due to their ease of fabrication and upkeep. They differ from typical devices in that they don't have any moving parts or components and don't use any dangerous chemicals or refrigerants [3-5]. Additionally, the thermoacoustic refrigeration systems' current applications are limited by their lower performance when compared to vapor compression refrigeration systems, i.e., they only attain Carnot efficiency at 14% to 19%, compared to 32% to 43% for the latter [6].

An acoustic driver produces sound energy, or a loudspeaker, in a refrigerator that operates on the thermoacoustic principle. The picture below depicts a standing wave thermoacoustic refrigeration system that is powered by a loudspeaker (Figure 1a). The system is composed of a loudspeaker, a resonating tube, heat exchangers, a stack, and an inert working medium, usually air. The gas packets inside the resonating tube expand and compress isentropically as the loudspeaker sustains a standing acoustic wave at its distinctive fundamental frequency.

At approximately a certain depth of thermal penetration into the stack, the thermal interface with the acoustical wave's initial temperature fluctuations are regulated by the stack, both in phase and magnitude. Along with an increase in the wave's temperature and pressure, heat is transmitted between the medium and the plate, which furthers the displacement of the gas fluid package towards the pressure antinode (Figure 1b). Pressure and temperature are reduced once the gas fluid parcel grows, and heat is then conveyed from the plate back to the gaseous fluid [7, 8]. Heat energy is transferred by one gas fluid packet and is deposited on the plate, and the same quantity of heat is then transferred by the next packet, resulting in the emergence of a temperature difference ΔT along the stack because a large number of gas fluid packets fluctuating in the stack towards the location of the thermal dissemination depth of the plate (Figure 1c) [9-10]. To take benefit of the effect of temperature difference established for the heat pumping operation, heat exchangers are mounted to the cold side and hot side of the stack. When cooling a low-temperature location, the cold edge heat exchanger absorbs heat, while the hot edge heat exchanger rejects heat to the environment [11, 12].

Several important aspects have an impact on the thermoacoustic refrigeration system's performance, including density, heat capacity of the operational fluid, thermal conductivity, and stack material. Resonance frequency, mean temperature and pressure, cooling load, and physical design restraints including position of stack, length of stack, and stack porosity are additional operating parameters. The performance of thermoacoustic systems has recently been the subject of extensive theoretical and experimental research efforts aimed at enhancing and optimizing it. The geometric design characteristics, particularly the stack, have been the subject of the majority of the analysis [13]. Tijani et al. [13] researched the best stack position for the parallel plate stack's geometry.

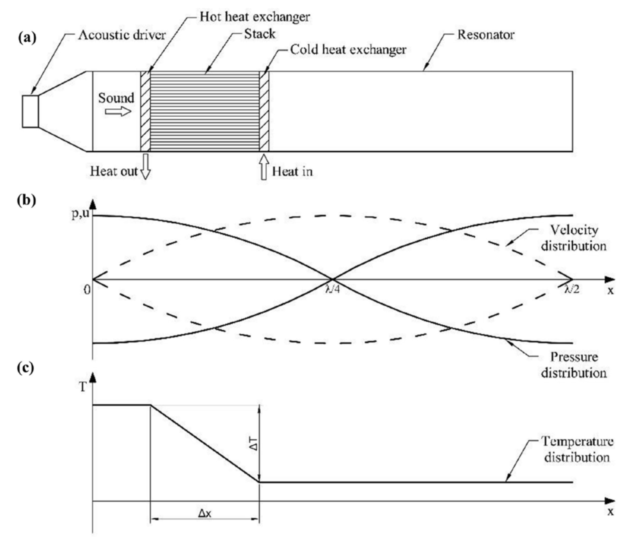

Figure 1: Working Principle of the thermoacoustic standing-wave refrigerator with pressure, velocity, and temperature distribution.

The results suggest that between 2 and 4 thermal penetration depths is the ideal range for the gap between the plates. Additionally, some preliminary testing was done on several stack designs, such as spiral-and honeycomb-shaped ones. Consideration was given to the consequence of stack material, length calculation, and position on temperature difference produced across the ends of the stacks [14]. The highest temperature differential was obtained with a 0.04 m corning Celor stack located 0.04 m from the speakers. Numerous testings were run, notably on the stack area. The ideal stack placement was computed using the temperature gradient and coefficient of performance (COP) [12, 15].

The effective range typically is between $\lambda/8$ and $\lambda/20$, where λ denotes the sound wavelength [9]. In a study by Picollo and Wetzel [14, 16] on the influence of the resonating tube and the operation of the stack, a good match between the resonating frequency and the resonating tube length results in a rise in the temperature divergence between the stacks two ends of around 55%. It was demonstrated that the ideal effective resonant frequency deviates from the plan under the assumption that $f_0 = a / (2L_0)$. Similar to this, Wetzel et al. [16] showed that the resonating frequency is significantly influenced by the length of the resonating tube, and in their estimations, the frequency decreased as the length of the resonator tube increased.

The review under discussion looks into how the size of the resonating tube and various operating frequencies affect how the thermoacoustic refrigeration system functions. In referenced boundaries, a model thermoacoustic refrigeration system with air as the working fluid was created. This system was operated by a loudspeaker connected to the amplifier through the signal generator. The experimental device was modified without the hot and cold heat exchangers. The thermoacoustic impact was computed specifically based on the temperature variance produced throughout the stack.

Experimental Setup and Details

The exploratory thermoacoustic system is shown in figure 2 as a schematic. The thermoacoustic refrigeration system did not include a cold and hot heat exchanger because the device was merely employed to measure the difference in temperature stimulated between the stack's two ends. The input acoustic device used to create the standing acoustic wave of the necessary frequency was a commercial amplifier-driven loudspeaker with 50 W of constant power. One end of the stack, which was also connected to the resonance tube and the buffer volume, held the acoustic loudspeaker. At the two ends of the stack, there were chambers with hot and cold temperatures. The material of the stack is permeable, the material and the stack's geometry were both made of Mylar with round pores. The temperature gradient that was formed between the two ends of the stack was brought on by exchanges among the fluid and the stack

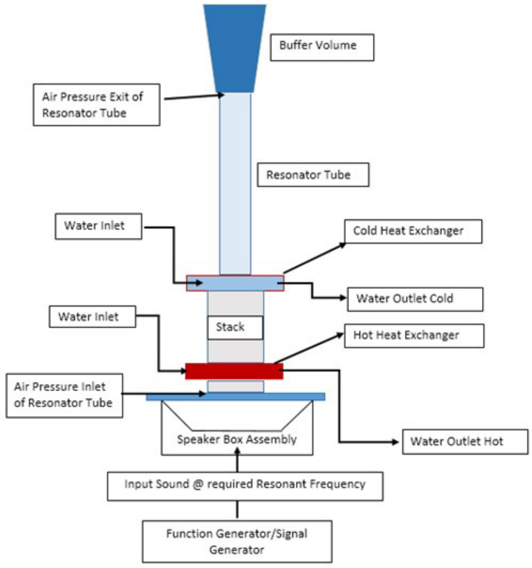

Figure 2: Schematic illustration of experimental setup.

material, as seen by the type-T digital thermocouple. A 1 K accuracy was used to display the temperature measurements at each end of the stack. After taking into consideration all key aspects that have a substantial impact on performance, the experimental data's overall precision and accuracy are in the 10% to 15% range.

The investigations were designed to estimate how well the thermoacoustic refrigeration system operated at various working frequencies and pressures. Equation (1) can be used to get the resonant frequency that is contingent on the length of the resonating tube and the speed of sound in air as the operating medium.

$$f0 = \frac{C}{4*L} \tag{1}$$

Length of Resonating Tube (Lt): 195 mm = 0.195 m
Length of Stack (Ls): 80 mm = 0.080 m
Total Length of the resonating medium (L):
Therefore, L = Lt + Ls
Considering, Lt = 195 mm = 0.195 m and Ls = 80 mm = 0.080 m,
L = Lt + Ls = 0.195 m + 0.080 m = 0.275 m

Speed of Sound in air : C
Ambient Temperature : Ta = 298 K
Gas Constant for air : R = 287 J/KgK
Adiabatic Index for Air : γ = 1.4

The velocity of sound in air is calculated using the Equation (2) given below with the above values specified.

$$C = \sqrt{\gamma * R * Ta} = 346\ m/s \tag{2}$$

The resonating frequency is now calculated for the fixed value of the resonating length (L = 0.275 m) for the first three fundamental modes of resonating wavelength i.e., (λ/4), (3λ/4), and (5λ/4) using the relation.

Figure 3: Experimental setup.

$$C = f0 * \lambda \tag{3}$$

Where,

L = (λ/4) corresponds to λ = (4L) (First Fundamental Quarter Wavelength Mode)

L = (3λ/4) corresponds to λ = (4L/3) (Second Fundamental Quarter Wavelength Mode)

L = (5λ/4) corresponds to λ = (4L/5) (Third Fundamental Quarter Wavelength Mode)

Substituting the above values of L in Equation (4), the three different resonating frequencies were calculated:

$f0$ = 294 Hz corresponds to λ = (4L) (First Fundamental Quarter Wavelength Mode)

$f0$ = 885 Hz corresponds to λ = (4L/3) (Second Fundamental Quarter Wavelength Mode)

$f0$ = 1474 Hz corresponds to λ = (4L/5) (Third Fundamental Quarter Wavelength Mode)

The resonant frequency is represented by f_0, the sound speed in air is represented by C, and the length of the resonating medium is represented by L. Three separate modes (λ/4), (3λ/4), and (5λ/4) needed for the creation of the standing acoustic wave were each assigned a resonant frequency estimate. Resonant frequencies for three distinct modes, f_0 = 294 Hz for (λ/4), f_0 = 885 Hz for (3λ/4), and f_0 = 1474 Hz for (5λ/4) were determined under the assumption that the length of the resonating medium (L) is constant. Data was gathered for each set of experimental measurements until it was demonstrated that the temperature distinction between the stack's ends was stable. In order to incorporate the comparison analysis with dependence on time, the experiment was run for a specified amount of time after the experiments had been done for the appropriate resonant frequency range. The experimental set up with all the parts attached together has been depicted in figure 2.

Results and Discussion

The various factors which have been considered for the comparative analysis of the experimental output have been depicted in the figures. Figure 4 shows the change of the temperature divergence produced within the stack at the resonant frequency of 294 Hz; the variation shows that as the compressed air in the system is increased from 1.5 bar to 3 bar, the temperature divergence within the stack likewise increases accordingly, even though nonlinear effects are present in some portions of the graph. The creation of acoustic sound velocity is not directly comparable to the mean average pressure of the medium, in this case air present inside the resonating medium, which explains the non-linearity effect. Similar to this, figure 5 and figure 6 illustrate, respectively, the experimental results for the change of the temperature differential generated throughout the stack at the resonant frequencies of f_0 = 885 Hz for (3λ/4) and f_0 = 1474 Hz for (5λ/4). Higher resonant frequencies demonstrated a similar pattern of performance. When acoustic sound power is applied to the system, a temperature contrast between the cold edge and hot edge of the stack begins to develop. The temperature disparity between the ends of the stack is seen to increase as system pressure increases in all of the aforementioned graphs and experimental results. The results of the experiment make it abundantly evident that the temperature modification produced throughout the stack is mostly proportional to the fluid pressure within the system. Furthermore, the highest temperature modification across the stack of 7.5 ˚C was obtained at a pressure of 3 bar for a resonant frequency of f_0 = 1474 Hz, the highest temperature change within the stack of 7.0 ˚C was obtained at 3 bar pressure for a resonant frequency of f_0 = 885 Hz, and the highest temperature alteration across the stack of 6.5 ˚C was obtained at 3 bar pressure for a resonating frequency of f_0 = 294 Hz.

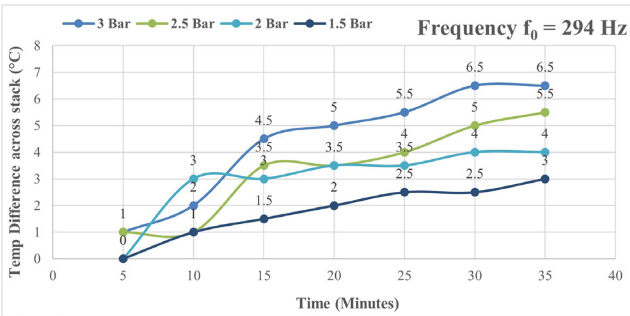

Figure 4: Temperature difference variation with time at f_0 = 294 Hz.

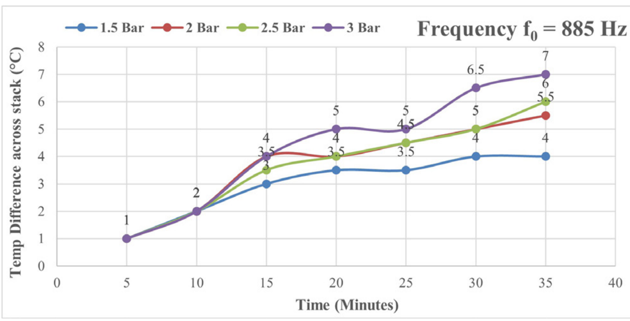

Figure 5: Temperature difference variation with time at f_0 = 885 Hz.

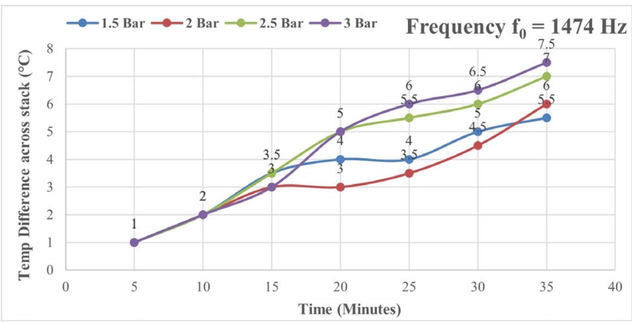

Figure 6: Temperature difference variation with time at f_0 = 1474 Hz.

Conclusion

In this experimental analysis, it was expected that the effective medium, air, would have an impact on the standing wave thermoacoustic refrigeration system's presentation with changing resonance frequencies and pressures. In order to analyze the temperature disparity between the stack's ends, three distinct resonating frequencies, corresponding to f_0 = 294 Hz for (λ/4), f_0 = 885 Hz for (3λ/4), and f_0 = 1474 Hz for (5λ/4) were taken into consideration. According to the results of the experiment, the thermoacoustic refrigeration system's operation is influenced by both the working medium's pressure and resonant frequency, in this case, air. The results also demonstrate that higher resonant frequencies result in the greatest temperature disparities across the stack. The length, working medium, stack size, shape, and geometry of the resonator tube, as well as other variables, can all be changed to conduct different investigations.

Acknowledgements

None.

Conflict of Interest

No conflict of interests that are significant to the article's content have been disclosed by the authors.

References

1. Swift G. 1996. Thermoacoustic engines and refrigerators. *Phys Today* 48(7).
2. Tijani MEH, Zeegers JCH, De Waele ATAM. 2002. Construction and performance of a thermoacoustic refrigerator. *Cryogenics* 42(1): 59-66. https://doi.org/10.1016/S0011-2275(01)00180-1
3. Hariharan NM, Sivashanmugam P, Kasthurirengan S. 2013. Experimental investigation of a thermoacoustic refrigerator driven by a standing wave twin thermoacoustic prime mover. *Int J Refrig* 36(8): 2420-2425. https://doi.org/10.1016/j.ijrefrig.2013.04.017
4. Reid RS, Swift GW. 2000. Experiments with a flow-through thermoacoustic refrigerator. *J Acoust Soc Am* 108(6): 2835-2842.

5. Basir Jafari S, Abolhassani MR, Amjadi A. 2008. Acousto-refrigerator with an adjustable mechanical resonator (research note). *Int J Eng* 21(2): 183-196.
6. Nsofor EC, Ali A. 2009. Experimental study on the performance of the thermoacoustic refrigerating system. *Appl Therm Eng* 29(13): 2672-2679. https://doi.org/10.1016/j.applthermaleng.2008.12.036
7. Wetzel M, Herman C. 2000. Experimental study of thermoacoustic effects on a single plate part I: temperature fields. *Heat Mass Transfer* 36(1): 7-20. https://doi.org/10.1007/s002310050358
8. Paek I, Mongeau L, Braun JE. 2010. Performance characterization of a small-capacity thermoacoustic cooler for air-conditioning applications. *J Mech Sci Technol* 24: 1781-1791. https://doi.org/10.1007/s12206-010-0610-2
9. Piccolo A. 2013. Optimization of thermoacoustic refrigerators using second law analysis. *Appl Energy* 103: 358-367. https://doi.org/10.1016/j.apenergy.2012.09.044
10. Tasnim SH, Mahmud S, Fraser RA. 2012. Effects of variation in working fluids and operating conditions on the performance of a thermoacoustic refrigerator. *Int Commun Heat Mass Transfer* 39(6): 762-768. https://doi.org/10.1016/j.icheatmasstransfer.2012.04.013
11. Jin T, Chen GB, Wang BR, Zhang SY. 2003. Application of thermoacoustic effect to refrigeration. *Rev Sci Inst* 74(1): 677-679.
12. Jebali F, Lubiez JV, François MX. 2004. Response of a thermoacoustic refrigerator to the variation of the driving frequency and loading. *Int J Refrig* 27(2): 165-175. https://doi.org/10.1016/S0140-7007(03)00100-2
13. Tijani MEH, Zeegers JCH, De Waele ATAM. 2002. Design of thermoacoustic refrigerators. *Cryogenics* 42(1): 49-57. https://doi.org/10.1016/S0011-2275(01)00179-5
14. Piccolo A, Cannistraro G. 2002. Convective heat transport along a thermoacoustic couple in the transient regime. *Int J Therm Sci* 41(11): 1067-1075. https://doi.org/10.1016/S1290-0729(02)01393-5
15. Bailliet H, Lotton P, Bruneau M, Gusev V, Valière JC, et al. 2000. Acoustic power flow measurement in a thermoacoustic resonator by means of laser Doppler anemometry (LDA) and microphonic measurement. *Appl Acoust* 60(1): 1-11. https://doi.org/10.1016/S0003-682X(99)00046-8
16. Wetzel M, Herman C. 1997. Design optimization of thermoacoustic refrigerators. *Int J Refrig* 20(1): 3-21. https://doi.org/10.1016/S0140-7007(96)00064-3